European Congress on Computational Methods
in Applied Sciences and Engineering (ECCOMAS 2012)
J. Eberhardsteiner et.al. (eds.)
Vienna, Austria, September 10-14, 2012

FINITE ELEMENT AND B-SPLINE METHODS FOR ONE-DIMENSIONAL NON-LOCAL ELASTICITY

M. Malagù[1,2], E. Benvenuti[1] and A. Simone[2]

[1]Engineering Department, University of Ferrara
Via Saragat 1, I-44100 Ferrara, Italy
e-mail: mlgmcl@unife.it, bnvlne@unife.it

[2] Faculty of Civil Engineering and Geosciences, Delft University of Technology
Stevinweg 1, 2628 CN Delft, The Netherlands
e-mail: a.simone@tudelft.nl

Keywords: non-local elasticity, FEM, B-spline

Abstract. *Non-local elasticity theories have been intensively applied to a wide range of problems in physics and applied mechanics. Most applications are based either on the integro-differential constitutive law proposed by Eringen or on the gradient constitutive law developed by Aifantis and co-workers. In this work, we study a one-dimensional non-local elastic tensile rod using Eringen and Aifantis constitutive laws. The problem is solved by means of standard finite elements and B-splines elements with high continuity. The results are compared with the C^{∞} analytical solution of the problem.*

1 INTRODUCTION

Growing interest in nanotechnology has fuelled the study of nanostructures such as nanotrusses. Classical continuum mechanics cannot fully describe the mechanical behavior of these structures due to the absence of an internal material length scale in the constitutive law. Since the works of Tupin [1] and Mindlin [2], higher-order gradient terms and internal length scale parameters have allowed the study of size effects at micro- and nanoscale. Eringen studies on non-local elasticity introduced integro-differential constitutive equations to account for the effect of long-range interatomic forces [3]. Furthermore, Aifantis and coworkers developed a strain gradient theory [4] in which microscale deformation is introduced by means of a higher-order strain tensor in the governing equations.

The numerical approximation of Eringen and Aifantis models is demanding. Non-local elasticity leads to high computational cost because of the integral form of the constitutive equations. On the other hand, the higher order derivatives in the governing differential equations of the strain gradient model stems into a higher number of boundary conditions and complicates discretization procedures due to higher-continuity requirements on finite element shape functions [5].

Recently, Isogeometric Analysis [6] has emerged as an innovative discretization technique for modeling complex geometries using shape functions employed in the Computer Aided Design community, namely B-splines and Non-Uniform Rational B-splines (NURBS). Main features of the Isogeometric Analysis approach are the geometry generation step and the *k*-refinement process in which the polynomial order and the continuity of the basis functions are likewise increased. Here we propose the use of higher-order B-spline basis functions for the study of one-dimensional nanotruss.

2 CONSTITUTIVE EQUATIONS

In an isotropic and homogeneous rod with Young's modulus E and cross sectional area A, Eringen non-local elasticity theory defines the stress σ at point x as a non-local function of the strain ε at surrounding points $\bar{x}$ [3]. In the present work, we adopt the following constitutive law proposed by Eringen [7] and later investigated, among others, by Polizzotto [8]:

$$\sigma(x) = E\xi_1\varepsilon(x) + E\xi_2 \int_\Omega \alpha(x,\bar{x})\, E\, \varepsilon(\bar{x})\, \mathrm{d}\bar{x}, \tag{1}$$

where the non-local modulus

$$\alpha(x,\bar{x}) = g_0\, e^{-\frac{|x-\bar{x}|}{\ell}} \tag{2}$$

is a weighting function in which the normalization factor $g_0 = (2\ell)^{-1}$ and ℓ is the material characteristic length. The two constitutive parameters ξ_1 and ξ_2 obey the relation $\xi_1 + \xi_2 = 1$ [9]. We also consider the Aifantis strain gradient constitutive law [4]

$$\sigma(x) = E\big(\varepsilon(x) - g^2\, \nabla^2\varepsilon(x)\big), \tag{3}$$

where g represents the material length related to the volumetric elastic strain energy. It can be shown [9] that setting $g = \ell\sqrt{\xi_1}$ leads to a strain gradient stress-strain law which turns out to be equivalent to the integral stress-strain relation (1) when a tensile rod subjected to constant stress is considered.

3 GOVERNING EQUATIONS

Governing equations for Eringen (1) and Aifantis (3) models are derived by setting the first variation of the total potential energy

$$\Pi(u) = W_i(u) - W_e(u) \tag{4}$$

equal to zero. In this expression, u is the axial displacement and W_i and W_e are, respectively, the virtual work of internal and external forces.

According to [8], the total potential energy corresponding to the integro-differential constitutive equation (1) is

$$\Pi^{nl}(u) = \frac{1}{2}\int_0^L \left[\xi_1 EA\varepsilon^2(x) + \frac{\xi_2\varepsilon(x)}{2\ell}\int_0^L e^{-\frac{|x-\bar{x}|}{\ell}} EA\varepsilon(\bar{x})\,\mathrm{d}\bar{x}\right]\mathrm{d}x - \int_0^L q(x)u(x)\,\mathrm{d}x, \tag{5}$$

where $q(x)$ is the distributed axial load. Setting $\varepsilon = u'$ and using the divergence theorem, the first variation

$$\begin{aligned}\delta\Pi^{nl}(u) = &-\int_0^L \left[EA\left(\xi_1 u''(x) + \frac{\xi_2}{2\ell}\int_0^L e^{-\frac{|x-\bar{x}|}{\ell}} u''(\bar{x})\,\mathrm{d}\bar{x}\right) + q(x)\right]\delta u(x)\,\mathrm{d}x \\ &+ \left[EA\left(\xi_1 u'(x) + \frac{\xi_2}{2\ell}\int_0^L e^{-\frac{|x-\bar{x}|}{\ell}} u'(\bar{x})\,\mathrm{d}\bar{x}\right)\delta u(x)\right]_0^L = 0\end{aligned} \tag{6}$$

for any δu. The second term in $\delta\Pi^{nl}$ vanishes due to the application of the boundary conditions and therefore, owing to the arbitrariness of δu, the governing equation for the non-local tensile rod reads

$$EA\left(\xi_1 u''(x) + \frac{\xi_2}{2\ell}\int_0^L e^{-\frac{|x-\bar{x}|}{\ell}} u''(\bar{x})\,\mathrm{d}\bar{x}\right) + q(x) = 0. \tag{7}$$

Following [10], the total potential energy for the strain gradient model is

$$\Pi^{g}(u) = \frac{1}{2}\int_0^L EA\big(\varepsilon(x) - g^2\nabla^2\varepsilon(x)\big)\varepsilon(x)\,\mathrm{d}x + \Big[\mu(x)\varepsilon(x)\Big]_0^L - \int_0^L q(x)u(x)\,\mathrm{d}x, \tag{8}$$

where $\mu(x)$ is the higher-order stress tensor defined by the constitutive equation

$$\mu(x) = g^2\, E\, \nabla\varepsilon(x). \tag{9}$$

From the first variation of (8) we have

$$\begin{aligned}\delta\Pi^{g}(u) = &-\int_0^L \big[EA\big(u''(x) - g^2 u''''(x)\big) + q(x)\big]\delta u(x)\,\mathrm{d}x \\ &+ \Big[EA\big(u'(x) - g^2 u'''(X)\big)\delta u(x) + g^2 EA u''(x)\delta u'(x)\Big]_0^L,\end{aligned} \tag{10}$$

which, as seen for the previous case, leads to the governing equation of the strain gradient rod

$$EA\big(u''(x) - g^2 u''''(x)\big) + q(x) = 0. \tag{11}$$

4 NUMERICAL DISCRETIZATION OF THE PROBLEMS

The numerical solution is next studied by means of standard finite elements and B-spline elements. The displacement field $u(x)$ and the axial strain $\varepsilon(x)$ are approximated at the element level through

$$u^e(x) \simeq \mathbf{N}_p^e(x)\,\mathbf{u}^e \qquad \text{and} \qquad \varepsilon^e(x) \simeq \frac{d\mathbf{N}_p^e}{dx}\,\mathbf{u}^e = \mathbf{B}_p^e(x)\,\mathbf{u}^e, \tag{12}$$

where $\mathbf{N}_p^e$ is a vector containing polynomial element basis functions of order p and $\mathbf{u}^e$ is the vector of the unknown displacement degrees of freedom. In the non-local case, the global stiffness matrix of the rod reads

$$\mathbf{K}^{nl} = \mathop{\mathsf{A}}_{e=1}^{n_{el}} \int_{x_1^e}^{x_1^e} \left(\xi_1\, \mathbf{B}_p^{eT}(x)\, EA\, \mathbf{B}_p^e(x)\, \mathrm{d}x + \frac{\xi_2}{2\ell} \int_0^L e^{\frac{|x-\bar{x}|}{\ell}}\, \mathbf{B}_p^{eT}(x)\, EA\, \mathbf{B}_p^e(\bar{x})\, \mathrm{d}\bar{x} \right) \mathrm{d}x, \tag{13}$$

whereas for the strain gradient formulation we have

$$\mathbf{K}^{g} = \mathop{\mathsf{A}}_{e=1}^{n_{el}} \int_{x_1^e}^{x_1^e} \left(\mathbf{B}_p^{eT}(x)\, EA\, \mathbf{B}_p^e(x) + g^2 \mathbf{C}_p^{eT}(x)\, EA\, \mathbf{C}_p^e(x) \right) \mathrm{d}x, \tag{14}$$

where $\mathbf{C}_p$ is a matrix containing global second derivatives of $\mathbf{N}_p$.

The integro-differential formulation is computationally burdensome since the computation of the elemental stiffness matrices requires the evaluation of stiffness contribution from the whole domain. Similarly, the computation of the stiffness matrix (14) for the strain gradient case is complicated by the higher continuity requirements for the displacement field interpolation. This problem can be solved by, for instance, using C^1 Hermite finite elements, the element-free Galerkin method, or staggered approaches [5] —unlike C^0 Lagrange function, increasing polynomial order in Hermite basis functions translate into increasing inter-elemental continuity as shown in Figures 1(a)- (b).

We choose to consider B-spline basis functions as they appear especially suitable for the construction of higher-order basis functions. In particular, we want to exploit the fact that by increasing the number of the degrees of freedom and the polynomial order of B-spline basis functions –the so called k-refinement method [6]–, the continuity order increases. The use of B-splines leads to a homogeneous structure of highly continuous basis functions along the whole one-dimensional domain as shown in Figure 1(c). Robust and efficient algorithms to compute high-order NURBS and B-spline basis functions, thus their derivatives, are well known in the literature [11, 12].

5 RESULTS

The problem of an elastic rod in tension depicted in Figure 2 is here studied employing Eringen and Aifantis models. The analytical solution derived in [9] and shown in Figure 3 is the same for the two models if g is set equal to $\ell\sqrt{\xi_1}$. The boundary layer at the two ends increases by increasing the value of $|1-\xi_1|$ and becomes sharper by decreasing the value of the constant material characteristic length. Furthermore, if $\xi_1 < 1$, the strain energy associated with the non-local solution is larger than that predicted by the classical elasticity theory, whereas for $\xi_1 > 1$ we have the opposite trend which is in agreement with experimental results [13]. The imposition of boundary conditions, which is not discussed in the present paper, is treated in [9].

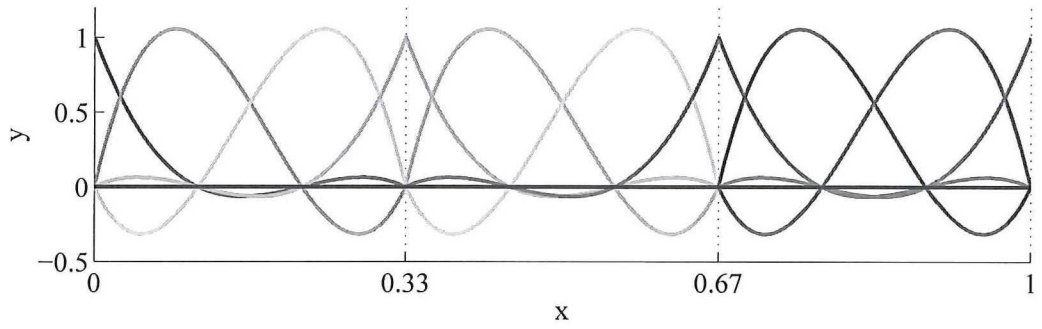

(a) Lagrange basis functions (p=3)

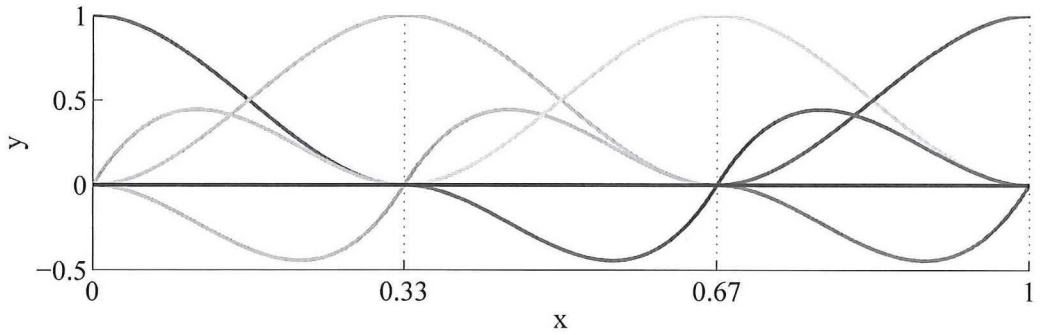

(b) Hermite basis functions (p=3)

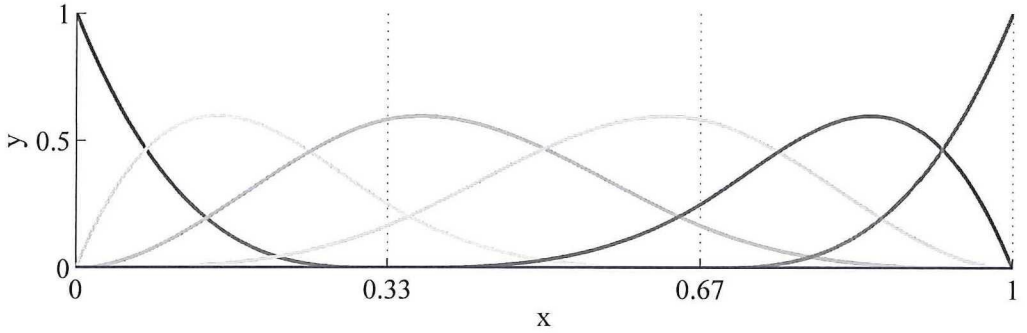

(c) B-spline basis functions (p=3)

Figure 1: One-dimensional domain descretized with three uniform elements and interpolated by means of cubic Lagrange, Hermite and B-spline basis functions.

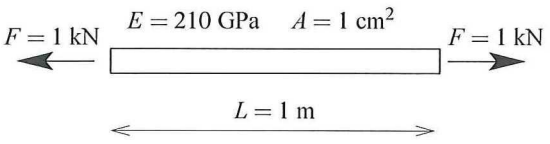

Figure 2: Homogeneous rod in tension.

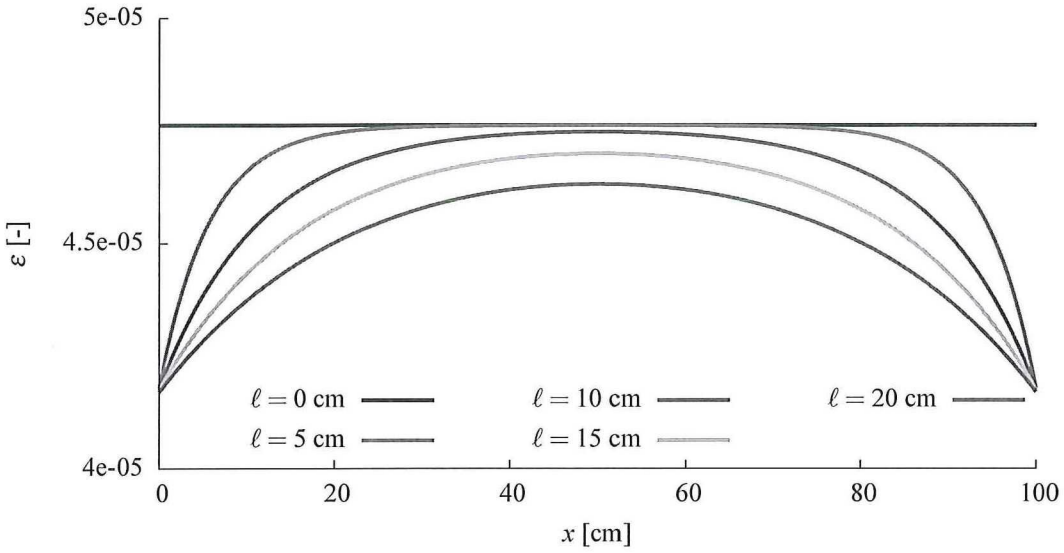

(a) $\xi_1 = 1.3$

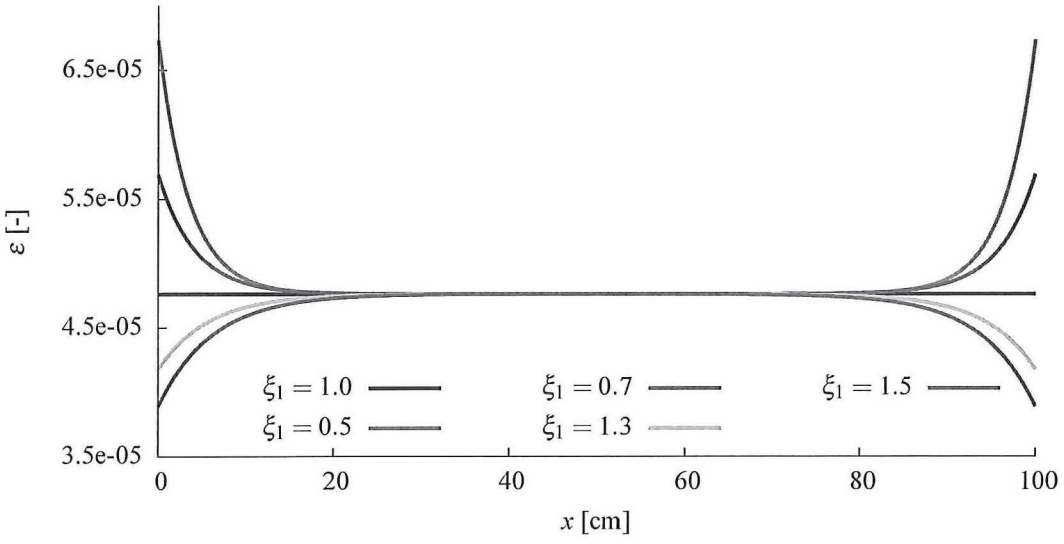

(b) $\ell = 5$ cm

Figure 3: The strain field in a nonlocal/gradient elasticity rod in tension.

Basis functions	Polynomial order	Continuity	Oscillations	Convergence
Lagrangian	2	C^0	no	bad
	3	C^0	yes	
	4	C^0	yes	
Hermite	3	C^1	yes	bad
	5	C^2	yes	
	7	C^3	yes	
B-spline	2	C^1	no	good
	3	C^2	no	
	4	C^3	no	

Table 1: Overview of the main features of the numerical solution obtained with Eringen formulation.

The numerical solution of the integral non-local model (1) obtained with Lagrange, Hermite and B-spline interpolations with 50 and 100 degrees of freedom is compared to the analytical solution in Figure 4. Figures 4(a) and 4(b) show that the strain field obtained with Lagrange basis functions is affected by oscillations along the whole domain which increase by increasing the polynomial degree. The oscillations decrease when Hermite basis functions are employed although they still persist along the whole domain and do not vanish by increasing the polynomial order (refer to Figures 4(c)-(d)). On the other hand, the wide support of the B-spline basis functions considerably improve the accuracy of the numerical solution. Figures 4(e) and 4(f) show that, by increasing the polynomial degree and, consequently, the continuity of the basis functions, the numerical solution improves.

The case of the strain gradient stress-strain law is next taken into account. The Lagrange interpolation is not feasible for this formulation due to the increased continuity requirements. Figure 5 reports the strain field obtained with the strain gradient model for Hermite and B-spline interpolations. In Figures 5(a) and 5(c), some oscillations appear at the boundaries when a very coarse discretization, 10 degrees of freedom, is adopted. The the numerical solutions obtained by means of Hermite and B-spline interpolations with 20 degrees of freedom are indistinguishable from the exact solution as shown in Figures 5(b) and 5(d).

The relative strain energy error for the non-local formulation in Figure 6(a) shows that the error associated with Hermite basis functions decreases slightly if compared to the C^0 Lagrange basis functions. The accuracy improves dramatically when B-spline basis functions are exploited —this seems to be related to the combined effect of the wide support and high-order continuity of B-spline basis functions. Figure 6(b) shows that the convergence rate increases significantly when the strain gradient formulation is discretized using Hermite and B-spline basis functions.

A summary of pros and cons of the adopted numerical procedures for the non-local and strain gradient formulations employed in this study is reported in Tables 1 and 2, respectively.

6 SUMMARY

The numerical solution of the problem of a tensile rod governed by non-local and strain gradient stress-strain laws is computationally burdensome. We employed Hermite and B-spline interpolations for both constitutive laws and Lagrange interpolation functions for the non-local model only. In the non-local case, the numerical results obtained by means of Lagrange and Hermite basis functions are affected by oscillations along the whole domain and exhibit slow

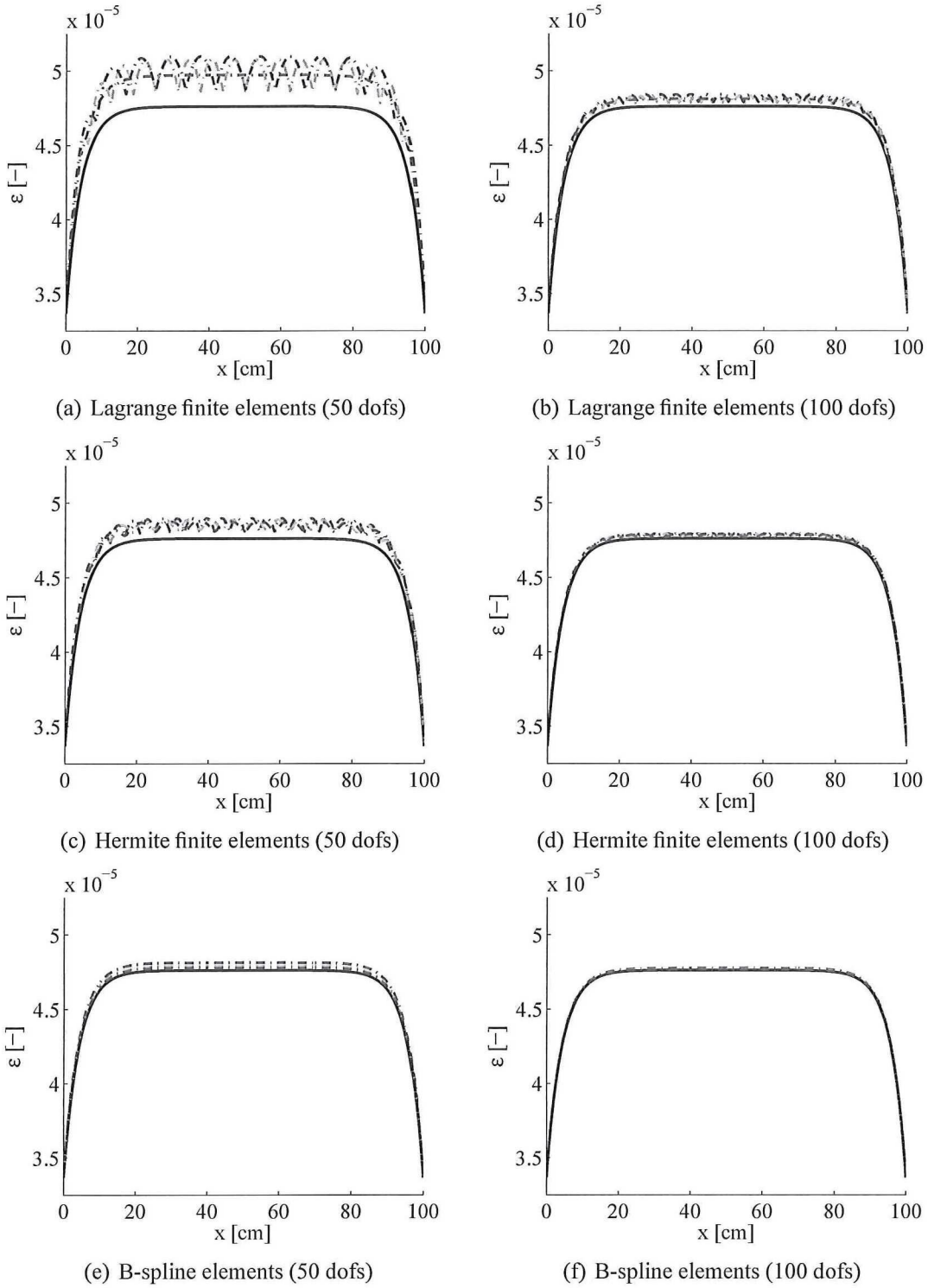

(a) Lagrange finite elements (50 dofs)

(b) Lagrange finite elements (100 dofs)

(c) Hermite finite elements (50 dofs)

(d) Hermite finite elements (100 dofs)

(e) B-spline elements (50 dofs)

(f) B-spline elements (100 dofs)

Figure 4: Tensile rod with Eringen formulation ($\xi_1 = 2$ and $\ell = 3$ cm). Exact solution (solid black line) and numerical solutions (dash-dot lines). Lagrange finite elements: quadratic (red), cubic (green) and quartic (blue) basis functions. Hermite finite elements: cubic (red), quintic (green) and septic(blue) basis functions. B-spline elements: quadratic (red), cubic (green) and quartic (blue) basis functions.

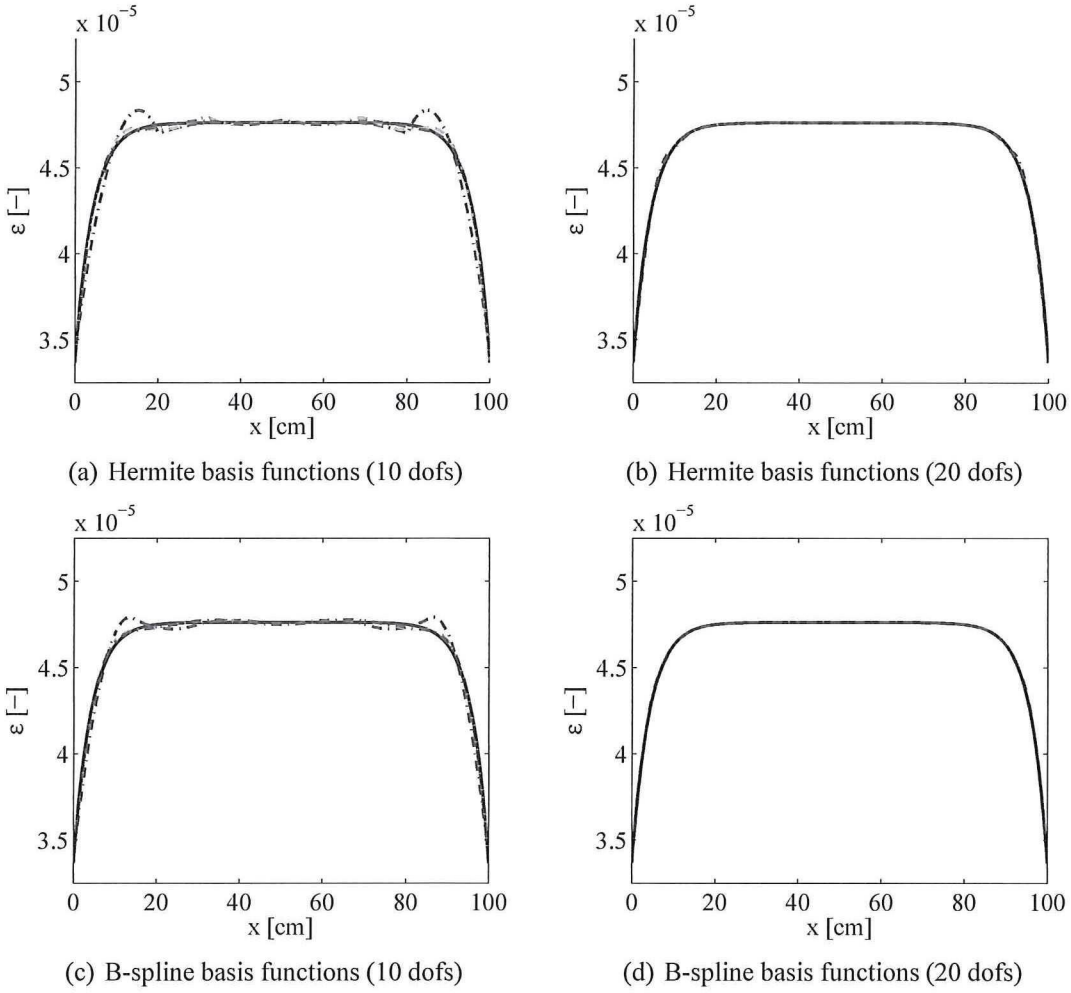

(a) Hermite basis functions (10 dofs)

(b) Hermite basis functions (20 dofs)

(c) B-spline basis functions (10 dofs)

(d) B-spline basis functions (20 dofs)

Figure 5: Tensile rod with Aifantis formulation ($g = \ell\sqrt{\xi_1} = 3\sqrt{2}$ cm). Exact solution (solid black line) and numerical solutions (dash-dot lines). Hermite finite elements: cubic (red), quintic (green) and septic (blue) basis functions. B-spline elements: quadratic (red), cubic (green) and quartic (blue) basis functions.

Basis functions	Polynomial order	Continuity	Oscillations	Convergence
Hermite	3 5 7	C^1 C^2 C^3	at the boundaries for few dofs	excellent
B-spline	3 5 7	C^2 C^4 C^6	at the boundaries for few dofs	excellent

Table 2: Overview of the main features of the numerical solution obtained with Aifantis formulation.

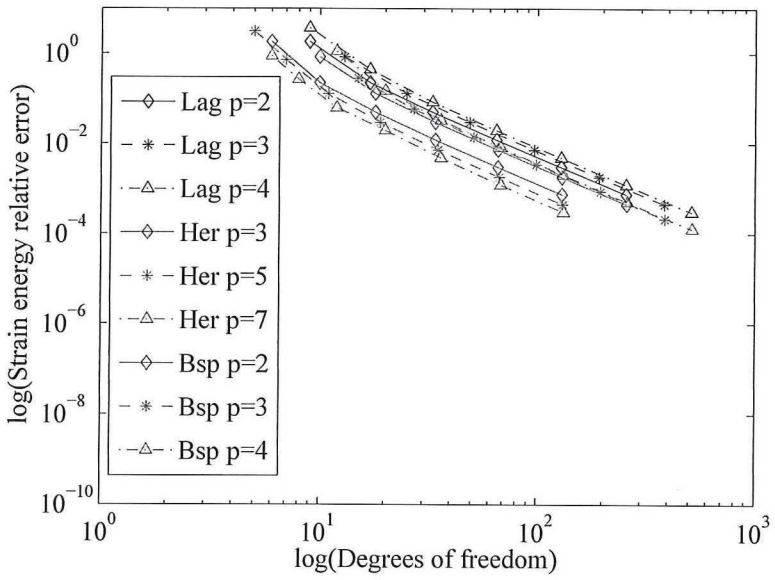

(a) Non-local formulation

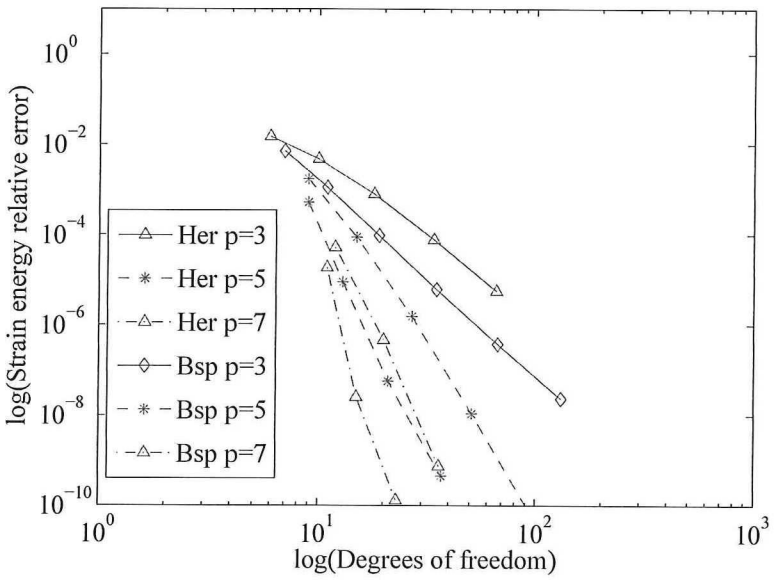

(b) Strain gradient formulation

Figure 6: strain energy convergence rate.

convergence in terms of strain energy relative error. Accuracy significantly improves when B-spline basis function are used. In the strain gradient case, Hermite and B-spline polynomials lead to almost equivalent results with reduced oscillations and improved strain energy convergence rate compared to the results obtained with the non-local model.

REFERENCES

[1] R. Tupin. Elastic materials with couple-stresses. *Archive for Rational Mechanics and Analysis*, 11:385–414, 1962.

[2] R. D. Mindlin. Micro-structure in linear elasticity. *Archive for Rational Mechanics and Analysis*, 16:51–78, 1961.

[3] A. C. Eringen. On differential equations of nonlocal elasticity and solutions of screw dislocation and surface waves. *Archive of Applied Mechanics*, 54:4703–4710, 1983.

[4] E. Aifantis. On the role of gradients in the localization of deformation and fracture. *International Journal of Engineering Science*, 30:1279–1299, 1992.

[5] H. Askes and E. C. Aifantis. Gradient elasticity in statics and dynamics: An overview of formulations, length scale identification procedures, finite element implementations and new results. *International Journal of Solids and Structures*, 48:1962–1990, 2011.

[6] T. J. R. Hughes, J. A. Cottrell, and Y. Bazilevs. Isogeometric analysis: CAD, finite elements, NURBS, exact geometry and mesh refinement. *Computer Methods in Applied Mechanics and Engineering*, 194:4135–4195, 2005.

[7] A. C. Eringen. *Nonlocal Continuum Field Theories*. Springer, 2001.

[8] C. Polizzotto. Nonlocal elasticity and related variational principles. *International Journal of Solids and Structures*, 38:7359–7380, 2001.

[9] E. Benvenuti and A. Simone. A unified analytical approach to one-dimensional nonlocal and gradient elasticity: Closed-form solution and size effect. Submitted for publication, 2012.

[10] I. Vardoulakis and J. Sulem. *Bifurcation Analysis in Geomechanics*. Chapman and Hall, 1995.

[11] L. A. Piegl and W. Tiller. *The NURBS Book*. Springer, 1997.

[12] C. de Falco, A. Reali, and R. Vázquez. Geopdes: A research tool for isogeometric analysis of pdes. *Advances in Engineering Software*, 42:1020–1034, 2011.

[13] W. D. Nix and H. Gao. Indentation size effects in crystalline materials: A law for strain gradient plasticity. 46:411–425, 1998.